Energy Scavenging for Inductively Coupled Passive RFID Systems

Bing Jiang, *Member, IEEE*, Joshua R. Smith, Matthai Philipose, Sumit Roy, *Fellow, IEEE*, Kishore Sundara-Rajan, and Alexander V. Mamishev, *Member, IEEE*

***Abstract*—Deployment of passive radio-frequency identification (RFID) systems or RFID-enhanced sensor networks requires good understanding of the energy scavenging principles. This paper focuses on the energy scavenging design considerations of inductively coupled passive HF RFID systems. The theoretical estimation of the power by a loop antenna is derived, and the effect of the design parameters on the harvested power is investigated. It is shown that the power delivery performance is largely affected by the tag load at the reader. An adaptive matching circuit at the reader is proposed for achieving optimum power delivery performance when the reader has a variable load. Experimental studies confirm analytical derivations.**

***Index Terms*—Antenna design, energy scavenging, impedance matching, loop antenna, passive tag, power harvesting, radio-frequency identification (RFID).**

I. Introduction

THE radio-frequency identification (RFID) technology is of growing interest to commerce, industry, and academia, especially due to the recent declines in cost and increases in read range because of improved design and associated signal processing. This technology can be used not only for identification, but also for tracking objects in a supply chain, monitoring the object's status, enhancing security, and many other applications [1].

The RFID system consists of readers/interrogators, tags/transponders, and an information managing host computer [2]. It operates in different frequency bands (e.g., 120 kHz, 13.56 MHz, 860–960 MHz, 2.45 GHz, and 5.8 GHz), while HF (13.56 MHz) and UHF (860–960 MHz) RFID are two mainstream technologies with well-established global standards. RFID tags can be categorized as: 1) active tag, which has a battery that supplies power to all functions; 2) semi-passive tag, which has a battery used only to power the tag IC, but not for communication; 3) passive tag, which has no battery on it. The absence of a power supply makes passive tags much cheaper and of much greater longevity than active tags.

As a low-cost wireless communication platform, the passive RFID system provides a possibility of implementing wireless sensor networks through integration of the RFID tag ICs and CMOS/microelectromechanical system (MEMS) sensors, as shown in Fig. 1. This proposed system is called here "the RFID-enhanced sensor system" [3], [4]. Such a system will not work well unless the enhanced tag receives enough energy from the reader. Successful energy scavenging in passive RFID systems will help in extending their applications. HF RFID uses magnetic waves in the antenna near field to communicate, while UHF uses electromagnetic waves. The operational range of HF RFID is from several centimeters to about a meter. Because the magnetic field is not affected by most of the surrounding dielectric materials ($\mu_r \approx 1$), HF RFID has good performance in a crowded environment when compared with UHF RFID. This paper focuses on the 13.56-MHz inductive passive HF RFID system.

Passive tags obtain impinging energy during reader interrogation periods, and the energy is used to power the tag IC. For the maximum read range, one has to ensure the maximum power transfer efficiency from the reader to the tag. What makes the problem challenging is that in the case of inductively coupled reader-tag, the reader must deal with a changing effective load due to 1) the location-dependent mutual coupling effect between the reader and tag and 2) the unpredictable number of tags in the read zone of the reader. Researchers have been working on optimum design of HF RFID. The general design issues in HF RFID were addressed, including read range in [5]. A tuning transformer for HF RFID was proposed for adjustment of resonant frequency [6]. However, the cause of over-coupling is not analyzed so far, and an easy and low-cost tuning method is needed to improve the energy delivery performance.

This paper presents a study of how mutual coupling between the reader and the tag affects the amount of power harvested at the tag. The mutual coupling can be viewed as a variable load at the reader. This load may lead to mismatch and poor power transfer efficiency if a fixed impedance matching circuit is implemented at the reader; accordingly, an adaptive impedance matching network at the reader is proposed. The antenna design guidelines to improve the power transfer from the reader to the tags are also presented.

II. Background

A. L-Match Network

Impedance matching is necessary in the design of RF circuitry in order to provide maximum power delivery between a source and its load and improve the signal to noise ratio of the system. Generally, an L-, T-, or π-matching network can be used to match the load to the source [7]. In this paper, the L-matching network is used due to its simplicity and ease of tuning. Fig. 2 shows the lumped circuits of the loop antenna only (left) and the

Manuscript received June 15, 2005; revised September 15, 2006.

B. Jiang, S. Roy, K. Sundara-Rajan, and A. V. Mamishev are with the Department of Electrical Engineering, University of Washington, Seattle, WA 98195 USA.

J. R. Smith and M. Philipose are with Intel Research, Seattle, WA 98105 USA.

Color versions of one or more of the figures in this paper are available online at http://ieeexplore.ieee.org.

Digital Object Identifier 10.1109/TIM.2006.887407

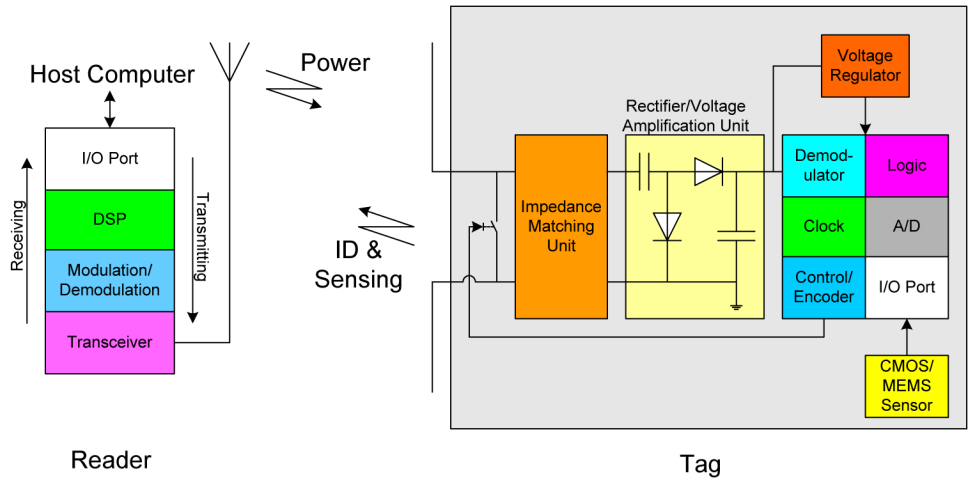

Fig. 1. RFID reader-tag (sensing node) system.

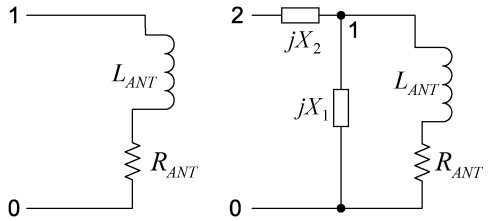

Fig. 2. L-matching network (left: original antenna; right: matched antenna).

loop antenna with the L-match network (right), where X_1 and X_2 are reactive elements for the matching purpose, and $R_{\rm ANT}$ and $L_{\rm ANT}$ are the resistance and self-inductance of the antenna. Fig. 2 is valid only when $|R_{\rm ANT} - j\omega L_{\rm ANT}| > R_{\rm sr}$, where $R_{\rm sr}$ is the source (generator) resistance [8], as shown in Fig. 5. This condition can be met in most cases. Thus, the impedance of an inductive antenna is matched to the source impedance as

$$jX_2 + \frac{(R_{\rm ANT} + j\omega L_{\rm ANT})jX_1}{R_{\rm ANT} + j\omega L_{\rm ANT} + jX_1} = R_{\rm sr} \tag{1}$$

where ω is the angular frequency. Due to the skin effect, $R_{\rm ANT}$ in (1) can be expressed as

$$R_{\rm ANT} \approx \frac{l}{2w}\sqrt{\frac{\pi f \mu}{\sigma}} \tag{2}$$

where σ and μ are the conductor's electrical conductivity and magnetic permeability, l is the length of the loop, w is the trace width, and f is the signal frequency [9].

It is difficult to accurately estimate $L_{\rm ANT}$ in (1), especially for a planar coil. For a round planar spiral coil $L_{\rm ANT}$ can be roughly approximated by (3) with at least 80% accuracy

$$L_{\rm ANT} \approx 31.33\mu N^2 \frac{a^2}{8a + 11c} \tag{3}$$

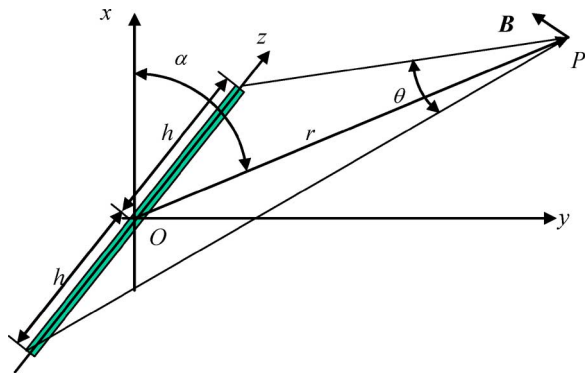

Fig. 3. Magnetic field generated by a dipole.

where N is the number of turns in the loop, a is the coil mean radius, and c is the thickness of the winding [10]. Analytical expressions for planar rectangular coils are available in [11]. Their accurate values can be approximated with numerical simulation software, such as HFSS. When the resistance and inductance of the loop are determined, X_1 and X_2 can be solved by using (1). In this paper, both X_1 and X_2 are implemented by capacitors (C_1 and C_2) due to the low cost.

B. Induced Magnetic Field

A changing current along a conductor loop induces a changing magnetic field. When another conductor loop is placed in this field, an induced voltage is generated. In order to simplify the calculation of the magnetic field, the loop can be treated as a series of small dipoles. Fig. 3 shows a dipole model. The magnetic field in the vicinity of the loop antenna is approximated as

$$\boldsymbol{B} \approx \frac{\mu_0 I_0}{2\pi} \frac{h}{r\sqrt{r^2 + h^2}} e^{j\omega t} \tag{4}$$

where h is the half length of the dipole, I_0 is the amplitude of the current along the loop, μ_0 is the permeability of air, and r is the distance from the location P (within the oxy plane) to the center of the dipole [12].

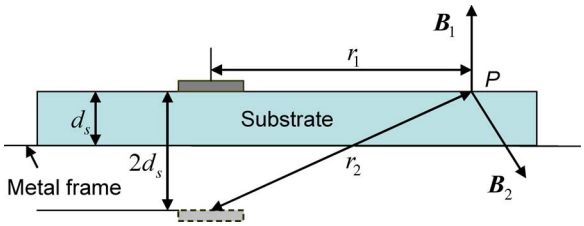

Fig. 4. Calculation model for the magnetic field of an antenna loop placed on a metal substrate with a certain distance.

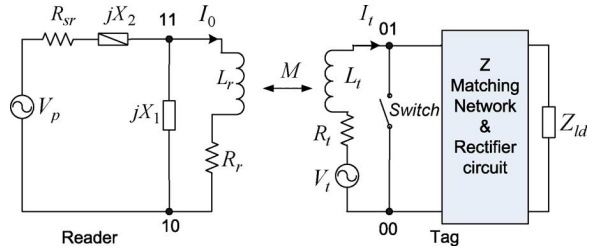

Fig. 5. Circuit schematics of the coupled RFID reader antenna and tag antenna.

Based on (4), the magnetic field along the central axis x generated by a rectangular loop antenna can be derived as

$$B_x = \frac{\mu_0 I_0}{2\pi} \sum_{i=1}^{n_r} \frac{x}{r_i \sqrt{r_i^2 + x^2}} \sin \alpha_i \tag{5}$$

where B_x is the amplitude of the magnetic field component along the x axis, n_r is the number of turns, and α is the angle between the line OP and the x axis, shown in Fig. 3. Further, B_x can be expressed in the geometrical parameters of the rectangular loop as

$$B_x = KI_0,$$
$$K \approx \frac{\mu_0}{\pi} \sum_{i=1}^{n_r} \frac{a_i b_i}{\sqrt{a_i^2 + b_i^2 + x^2}} \left(\frac{1}{a_i^2 + x^2} + \frac{1}{b_i^2 + x^2} \right) \tag{6}$$

where a_i and b_i are the half length of the i^{th} side.

We have assumed that loop antennas are surrounded by the air. However, a different magnetic field distribution occurs when antennas are placed on the top of a metal frame. Therefore, it is important to estimate the metal effect on the power transfer. We assume the antenna loop with a distance d_s to a metal frame. The image of the antenna loop under the frame plane has the exact distance d_s to the metal plane. Fig. 4 shows the configuration.

Since $B_x = B_{1x} + \cos(\delta) B_{2x}$, B_x is rewritten as

$$B_x = \frac{\sqrt{2}\mu_0 I_0}{4\pi} \left(r^{-1} + \cos(\delta) r \left(r^2 + (2d_s)^2 \right)^{-1} \right) \tag{7}$$

where $\cos(\delta) = -1$ if the dipole is perfectly parallel to the metal plane [8]. When d_s is small compared to r, the above equation is simplified as

$$B_x = \frac{1}{\pi} \sqrt{2} \mu_0 d_s^2 r^{-3} I_0 = KI_0. \tag{8}$$

C. Induced Voltage

When a loop is placed in the magnetic field, an induced voltage is calculated as

$$V_t = \int_C \boldsymbol{E} \cdot d\boldsymbol{l} = -\frac{\partial}{\partial t} \int_S \boldsymbol{B} \cdot d\boldsymbol{s} \tag{9}$$

where C is the length of the loop curve, S is the area of the loop, $\boldsymbol{E}$ is the electric field vector, $\boldsymbol{l}$ is the tangent direction of the loop curve, and $\boldsymbol{s}$ is the normal direction of the loop surface. Since the RFID tag is usually very small, $\boldsymbol{B}$ is treated as a constant at the tag location. Because the induced voltage from each turn is serially connected, for a tag with a n_t turn antenna the induced voltage is

$$V_t \approx -j\omega B \sum_{i=1}^{n_t} S_i = -j\omega I_0 K \sum_{i=1}^{n_t} S_i. \tag{10}$$

Equation (10) shows that V_t can be adjusted by tuning design parameters, such as the number of turns and the dimension of the loop. This approximation is based on the assumption that the magnetic field generated by the tag in the direction opposite to the magnetic field generated by the reader is negligible, i.e., I_0 is treated as a constant. When the reader antenna and the tag antenna are far apart, this assumption usually holds true. However, it cannot be used to accurately predict the output voltage when the tag works in the near field of the reader antenna. I_0 is forced to change in this case. In order to reach optimum power delivery, the accurate estimations of I_0 and V_t are required.

III. Loading Effect

The induced voltage on the tag generates current along the tag loop antenna, following an EM field in the direction opposite to the triggering EM field. The reader antenna and the tag antenna can be treated as a pair of weakly coupled transformers, as shown in Fig. 5 with a mutual coupling factor M [13]. Therefore, the induced voltage at the tag can also be derived as

$$V_t = j\omega M I_0. \tag{11}$$

According to (10), the coupling coefficient is determined as

$$M = -K \sum_{i=1}^{n_t} S_i. \tag{12}$$

Equation (12) shows that M is only determined by the geometry and the relative position of the two antennas.

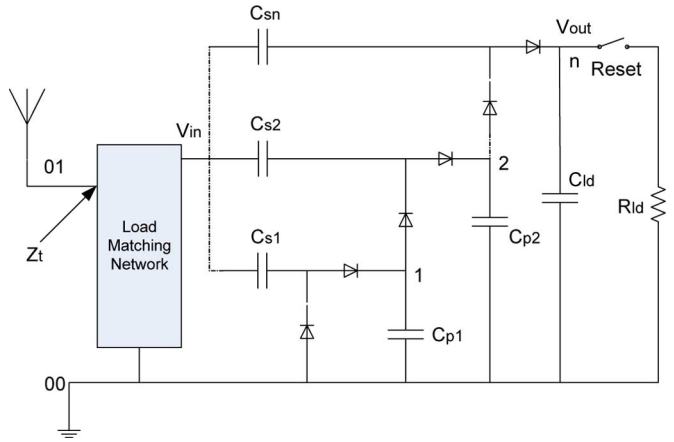

Fig. 6. Lumped circuit model for the rectifier circuit.

Based on the KVL and KCL, the following equations are derived for a RFID reader antenna when it is loading tags and is matched with an L-matching network:

$$\begin{cases} V_p = R_{\rm sr} I + Z_2 I + V_r \\ I = I_0 + \frac{V_r}{Z_1} \\ V_r = (R_r + j\omega L_r) I_0 + j\omega M I_t \end{cases} \tag{13}$$

where R_r and L_r are the resistance and inductance of the reader antenna, respectively; V_p and V_r are the driving source voltage and voltage at the reader antenna, respectively; I, I_0, and I_t are the current flowing through $R_{\rm sr}$, the reader antenna, and the tag antenna, respectively; and $Z_1 = jX_1$ and $Z_2 = jX_2$ are the impedances of the LC matching elements.

Using KVL for the tag circuit yields

$$j\omega M I_0 + (R_t + j\omega L_t) I_t + Z_t I_t = 0 \tag{14}$$

where R_t and L_t are the tag resistance and inductance, and Z_t is the tag impedance at the port 00-01, including the matching network, rectifier, and load impedance Z_{ld}, as shown in Fig. 5. The induced power on the tag is rectified and fed to the load. Fig. 6 depicts the rectifier circuit. More discussion on the rectifier design can be found in [14]–[16].

Ideally, the maximum output power can be reached when the load impedance is matched to the source impedance $(R_t + j\omega L_t)$. Relevant methods of complex impedance match for the RFID tag can be found in [17]. When matched, the tag impedance can be expressed as

$$Z_t = R_t - j\omega L_t. \tag{15}$$

Therefore, the current I_t is given by

$$I_t = -\frac{1}{2R_t} j\omega M I_0. \tag{16}$$

Replacing I_t in (13) by using (16), I_0 is expressed as

$$\left(1 + \left(\frac{2R_{\rm sr}(R_r + j\omega L_r + Z_1) + Z_1^2}{2R_{\rm sr}(R_r + j\omega L_r + Z_1)^2}\right)\frac{(\omega M)^2}{2R_t}\right) I_0 = \frac{Z_1}{R_r + j\omega L_r + Z_1}\frac{V_p}{2R_{\rm sr}}. \tag{17}$$

Here, I_0 is still unsolved, since L_r and Z_1 remain unknown. When the unloaded loop antenna $(M = 0)$ is matched to the source resistance $R_{\rm sr}$, the power dissipated by the antenna is

$$P_{\rm ANT} = \frac{1}{2}\left(\frac{1}{2}\frac{V_p^2}{2R_{\rm sr}}\right) = \frac{V_p^2}{8R_{\rm sr}}. \tag{18}$$

Since the passive elements do not dissipate power, $P_{\rm ANT}$ the power is the power dissipated by R_r, i.e.,

$$|I_{0\_\rm unload}| = \frac{V_p}{2R_{\rm sr}}\sqrt{\frac{R_{\rm sr}}{R_r}}. \tag{19}$$

When $M = 0$, I_0 can also be derived from (13) as

$$I_{0\_\rm unload} = \frac{V_p}{2R_{\rm sr}}\frac{Z_1}{R_r + j\omega L_r + Z_1}. \tag{20}$$

Referring to (19), $Z_1/(R_r + j\omega L_r + Z_1)$ can be simplified as

$$\frac{Z_1}{R_r + j\omega L_r + Z_1} = \sqrt{\frac{R_{\rm sr}}{R_r}} e^{j\vartheta} \tag{21}$$

where ϑ is the phase. Introducing (21) into (17) and $Z_1 = (1/j\omega C_1)$, (17) is rewritten as

$$\left(1 + \left(\omega C_1\sqrt{\frac{R_{\rm sr}}{R_r}} e^{j(\vartheta+\pi/2)} + \frac{1}{2R_r} e^{j2\vartheta}\right)\frac{(\omega M)^2}{2R_t}\right) I_0 = \sqrt{\frac{R_{\rm sr}}{R_r}} e^{j\vartheta}\frac{V_p}{2R_{\rm sr}}. \tag{22}$$

Since ωC_1 and ϑ in (22) are usually very small, this equation can be simplified as

$$I_0 \approx \sqrt{\frac{R_{\rm sr}}{R_r}}\frac{V_p}{2R_{\rm sr}}\left(1 + \frac{1}{4}\frac{(\omega M)^2}{R_r R_t}\right)^{-1}. \tag{23}$$

Therefore, the harvested power P_T on the RFID tag IC circuitry can be expanded from (18) as

$$P_T \approx \frac{1}{8R_t}\sqrt{\frac{R_{\rm sr}}{R_r}}\frac{V_p}{2R_{\rm sr}}\left|\omega M\left(1 + \frac{1}{4R_r R_t}(\omega M)^2\right)^{-1}\right|^2. \tag{24}$$

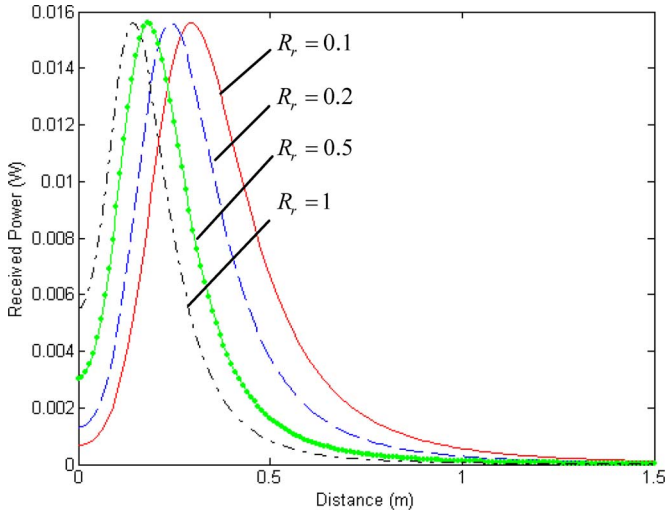

Fig. 7. Relationship between the received power and the coupling factor.

IV. Discussion

Equation (24) shows that there is a nonlinear relationship between P_T and M. Fig. 7 clearly demonstrates this nonlinear property, where the reader antenna has $S = 0.2 \times 0.2$ m^2 area and one turn, the tag antenna has $S = 0.023$ m^2 area and ten turns, $R_t = 6.2\ \Omega$, $V_p = 5$ V, and $R_{\rm sr} = 50\ \Omega$. The complex relationship between P_T and M can be simplified in two scenarios.

A. Small Load Effect

When $(\omega M)^2/(4R_rR_t) \ll 1$, P_T can be estimated as

$$P_T \approx \frac{1}{32R_tR_rR_{\rm sr}}(\omega V_p)^2|M|^2. \tag{25}$$

Equations (4), (6), and (12) also show that $|M| \propto 1/r$ in the near field, but $|M| \propto 1/r^2$ in the far field. This relationship indicates that the inductive RFID tags can only work in the near field of the reader antenna with a limited range. If a tag is located in the center of the square antenna, and R_r and R_t is replaced by using (2), P_T can be expressed as

$$P_T = \frac{f\mu}{256\pi R_{\rm sr}}V_p^2\frac{1}{h_r^3}\sigma w_r w_t n_r n_t h_t \tag{26}$$

where w_r and w_t are the trace width of the reader antenna and the tag antenna, h_r and h_t are the half side length of the reader antenna and the tag antenna, and σ and μ are the conductivity and permeability of the conductor. Equation (26) expresses the effect of design parameters on P_T.

Usually, an expected working range is prespecified as a design goal; therefore, determining the antenna size is important. For a square loop, (11) can be rewritten as

$$V_t = k_0\frac{h^2}{(r_d^2+h^2)\sqrt{r_d^2+2h^2}} \tag{27}$$

where k_0 is a constant, and r_d is the expected range. When $dV_t/dh = 0$, we can obtain the optimum half side length of the loop

$$h = \sqrt{\frac{1}{2}(1+\sqrt{5})}r_d. \tag{28}$$

For a circular loop, a small dipole can be approximated as

$$h \approx r_c\frac{\Delta\theta}{2} \tag{29}$$

where r_c is the radium of the circular loop, and θ is the sector angle to the cord $2h$, as shown in Fig. 3. B_x, and V_t can be expressed as

$$B_x = \frac{I_0\mu}{2\pi}\int_0^{2\pi}\frac{r_c^2}{2\left(r_d^2+r_c^2\right)^{3/2}}d\theta = \frac{I_0\mu}{2}\frac{r_c^2}{\left(r_d^2+r_c^2\right)^{3/2}} \tag{30}$$

$$V_t = k_0B_x = \frac{I_0\mu}{2}k_0r_c^2\left(r_d^2+r_c^2\right)^{-3/2}. \tag{31}$$

When $dV_t/dr_c = 0$, we can obtain the optimum radius of the loop

$$r_c = \sqrt{2}r_d. \tag{32}$$

When the loop is placed on the top of a metal shelf, according to (8), the mutual coupling M decreases because of the metal frame. Therefore, the loop antenna should be kept as far away from the metal frame as possible, and using a loop with a smaller size is preferred. The matching elements should be adjusted correspondingly to reach optimum power delivery performance, since the loop inductance has changed.

B. Large Load Effect

When $(\omega M)^2/(4R_rR_t) > 1$

$$P_T \approx V_p^2\frac{R_tR_r}{2R_{\rm sr}}\frac{1}{|\omega M|^2}. \tag{33}$$

It shows that P_T decreases as the coupling factor $|M|$ increases, because a larger coupling results in a smaller I_0. Two possible situations may result in large coupling: 1) many tags in the reader operating range and 2) a closely located tag. When a tag is moved closely to the reader, the output voltage may increase gradually until it peaks and then drops. In other words, a relatively large coupling effect could lower the power transfer between the reader and the tag, as shown in Fig. 7.

The degraded performance of power transfer can be a serious problem in power-hungry applications, such as RFID-enhanced sensor networks. An adaptive matching network that changes the reactive element values to match the changing load may be used to improve power transfer efficiency [18], [19]. However, the lack of a feasible feedback loop makes it difficult to implement. Fig. 8 shows that a modified matching circuit is used on the RFID reader antenna. The only drawback of this method is that the tag takes a longer time to respond to the reader's inquiry,

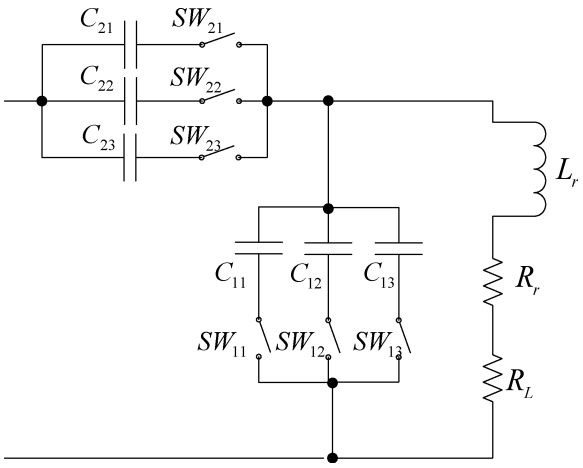

Fig. 8. Schematics of the adaptive L-match network.

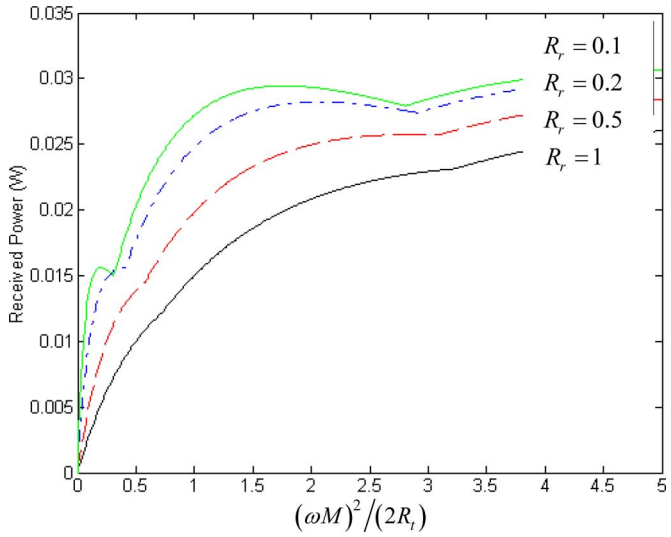

Fig. 9. Simulated result by using the adaptive L-match network.

since the reader needs more time to sweep different configurations. Fig. 9 shows the power delivery improvement over the fixed matching circuit. Based on the maximum power transfer with impedance matching, the power received by the tag when using the fixed matching algorithms shows a maximum value of 12.5% of $V_p^2(8R_{\rm sr})^{-1}$ which is the total power consumed. Fig. 9 shows the maximum power efficiency for the adaptive matching network can be reached to 25%.

V. Experimental Results

We designed a tag loop with 15 turns, 46×46 mm^2 outer dimensions, 0.254-mm gap, and 0.254-mm track width. We used a one-stage rectifier to rectify the signal. Figs. 10–12 show the experimental results with $V_p = 3$ V, where the x axis represents the distance between the centers of two antennas, and the y axis represents the output voltage generated on the tag. Experiments show that the output voltage can drop as the mutual coupling increases to certain levels. This effect is highly pronounced when the distance between the tag and reader is short, the size of the reader antenna is small (Fig. 10), or the loop turn number is large (Fig. 11). According to (12), (24), and (33), the increasing

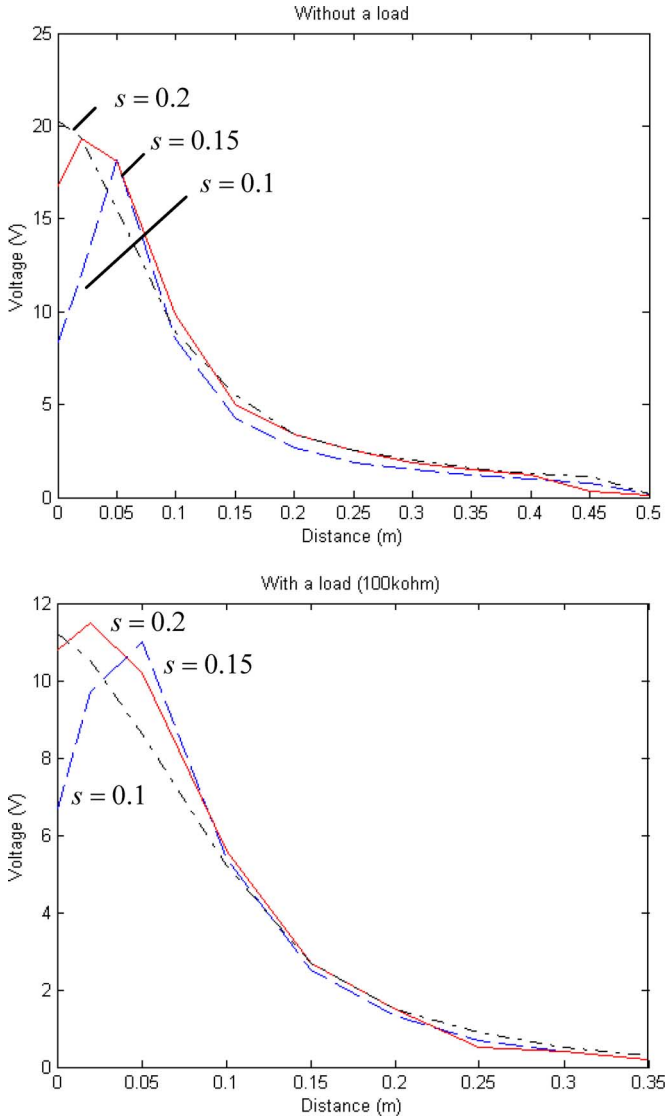

Fig. 10. Characteristics of inductive coupling in RFID systems (s—the side length of RFID reader antenna).

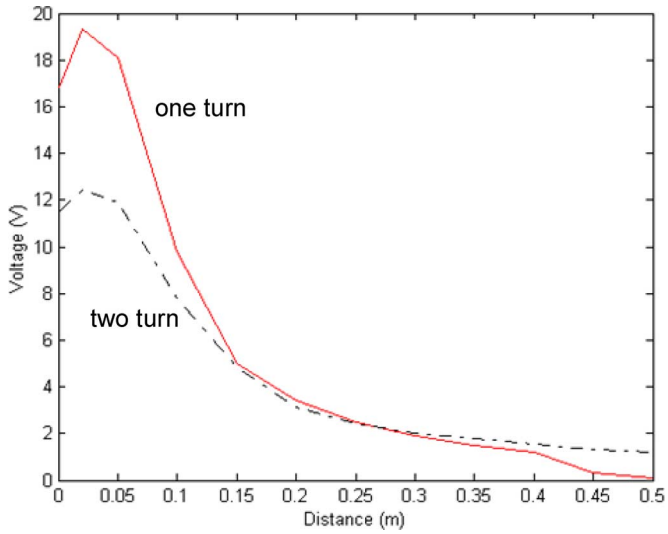

Fig. 11. Characteristics of inductive coupling in RFID systems-turn effect (the side length of reader antenna is 10 cm).

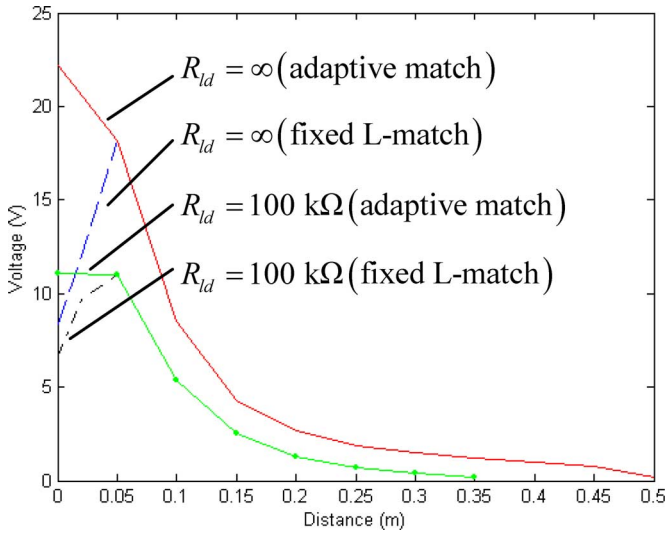

Fig. 12. Influence of adaptive matching (the side length of reader antenna is 10 cm).

mutual coupling factor can decrease the received power. The experimental results coincide with the theoretical analysis. Using an adaptive matching circuit optimizes the power transfer with a varying load. Fig. 12 shows the voltage generated as a function of distance between the tag and the reader at load levels for a fixed impedance matching circuit and an adaptive matching circuit. The adaptive matching circuit offers significant improvement when the over coupling exists. In the far field, both adaptive matching and fixed L impedance matching offer the same performance.

VI. Conclusion

An analytical method to compute the power delivered to the RFID tag as a function of the mutual coupling between the loop antennas of the tag and reader was introduced. The effect of the variable mutual coupling on the power delivery was discussed. An adaptive impedance matching circuit implemented on the reader antenna was proposed as a solution to mitigate the detrimental effect of the mutual load on the power transfer efficiency. The design procedure for HF loop antenna specifications was also given, including determinations of the loop size.

References

[1] V. Stanford, "Pervasive Computing Goes the Last Hundred Feet With RFID Systems," *IEEE Pervasive Comput.*, vol. 2, no. 2, pp. 9–14, Feb. 2003.
[2] K. Finkenzeller, *RFID Handbook: Fundamentals and Applications in Contactless Smart Cards and Identification*, 2 ed. New York: Wiley, 2003.
[3] M. Philipose, J. R. Smith, B. Jiang, A. Mamishev, S. Roy, and K. Sundara-Rajan, "Battery-free wireless identification and sensing," *IEEE Pervasive Comput.*, vol. 4, no. 1, pp. 37–45, Jan. 2005.
[4] R. Want, "Enabling ubiquitous sensing with RFID," *Computer*, vol. 37, no. 4, pp. 84–86, 2004.
[5] S. Chen and V. Thomas, "Optimization of inductive RFID technology," in *Proc. IEEE Int. Symp. Electronics and the Environment*, 2001, pp. 82–87.
[6] G. Steiner, H. Zangl, P. Fulmek, and G. Brasseur, "A tuning transformer for the automatic adjustment of resonant loop antennas in RFID systems," in *Proc. IEEE Int. Conf. Industrial Technology*, 2004, vol. 2, pp. 912–916.
[7] C. Bowick, *RF Circuit Design*. Burlington, MA: Newnes, 1997.
[8] D. Pozar, *Microwave Engineering*, 2nd ed. New York: Wiley, 2003.
[9] AN831: Matching Small Loop Antennas to rfPIC Devices, Microchip application notes, 2002.
[10] "Simple inductance formulas for radio coils," *Proc. IRE*, vol. 16, no. 10, 1928.
[11] H. Greenhouse, "Design of planar rectangular microelectronic inductors," *IEEE Trans. Parts, Hybrids, Packag.*, vol. 10, no. 2, pp. 101–109, Feb. 1974.
[12] J. Kraus, *Antennas*, 2nd ed. New York: McGraw-Hill, 1988.
[13] AN680: MicroID 13.56 MHz RFID System Design Guide, Microchip application notes, 2001.
[14] B. Jiang, "Ubiquitous Monitoring of Distributed Infrastructures," Ph.D. dissertation, Univ. Washington, Seattle, 2006.
[15] Z. Zhu, B. Jamali, and P. H. Cole, *Brief Comparison of Different Rectifier Structures for HF and UHF RFID (Phase I)*, Auto-ID Labs, 2004.
[16] ——, *Brief Comparison of Different Rectifier Structures for HF and UHF RFID (Phase II)*, Auto-ID Labs, 2004.
[17] P. V. Nikitin, K. V. S. Rao, S. F. Lam, V. Pillai, R. Martinez, and H. Heinrich, "Power reflection coefficient analysis for complex impedances in RFID tag design," *IEEE Trans. Microw. Theory Tech.*, vol. 53, no. 9, pp. 2721–2725, Sep. 2005.
[18] B. Nauta and M. B. Dijkstra, "Analog line driver with adaptive impedance matching," *IEEE J. Solid-State Circuits*, vol. 33, no. 12, pp. 1992–1998, Dec. 1998.
[19] M. Thompson and J. K. Fidler, "Application of the genetic algorithm and simulated annealing to LC filter tuning," *Proc. IEE, G—Circuits, Devices, Syst.*, vol. 48, no. 4, pp. 177–182, 2001.

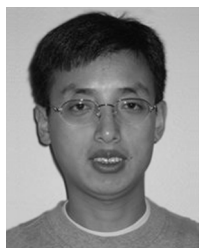

Bing Jiang (S'01–M'06) received the B.S. degree from Tianjin University, Tianjin, China, in 1995, and the M.S. and Ph.D. degrees in electrical engineering from the University of Washington, Seattle, in 2003 and 2006, respectively.

He was an intern at Intel Research Seattle from September 2003 to June 2004. Currently, he is a Senior RF Engineer at Vue Technology. He is the author of about 20 journal and conference papers. His research interests include RFID, robotics, and sensors.

Joshua R. Smith received the B.A. degrees in computer science and philosophy from Williams College, Williamstown, MA, the M.A. degree in physics from the University of Cambridge, Cambridge, U.K., and the M.S. and Ph.D. degrees from the Media Lab's Physics and Media Group, Massachusetts Insitute of Technology, Cambridge, MA.

He is a member of the research staff at Intel Research Seattle, Seattle, WA, and an affiliate Professor in the Departments of Electrical Engineering and Computer Science and Engineering, University of Washington, Seattle. His earlier work on electric field imaging is the basis of a passenger-side airbag suppression product deployed in Honda and GM automobiles. He also invented a physical document security technology called FiberFingerprint, and published an influential early paper on Digital Watermarking. He is the inventor or coinventor of nine issued U.S. patents.

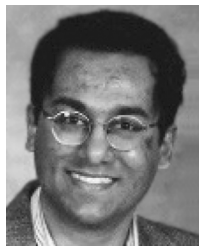

Matthai Philipose received the B.S. degree from Cornell University, Ithaca, NY, and the Ph.D. degree from the University of Washington, Seattle, both in computer science.

He leads the Human Activity Recognition project at Intel Research, Seattle. He builds systems that observe and reason human activity, emphasizing detailed, but tractable, models of activity, very high-density sensing, and automatically acquired commonsense. He is particularly interested in applying these systems to the problem of eldercare. He is broadly interested in statistical reasoning, logic, and programming languages.

Sumit Roy (F'07) is a Professor of electrical engineering, University of Washington, Seattle, and a Visiting Faculty Consultant to Intel Research, Seattle. His areas of technical interest involve wireless communication systems. He is currently exploring the use of RFID and 802.11 WLAN technologies within networked ubiquitous computing environments. He recently spent two years on academic leave at the Wireless Technology Development Group within Intel Labs, Hillsboro, OR, working on next-generation Wireless LAN and PAN systems.

Prof. Roy is an active member of the IEEE Communications Society.

Kishore Sundara-Rajan received the B.Eng. degree in electrical and electronics engineering from the University of Madras, India, in 2001, and the M.S. degree in electrical engineering from the University of Washington, Seattle, in 2003.

Since 2002, he has been a graduate research assistant at the Sensors, Energy, and Automation Laboratory, Department of Electrical Engineering, University of Washington. His research interests include sensor design and integration, MEMS, and dielectric spectroscopy.

He is a recipient of the IEEE-DEIS Graduate Fellowship.

Alexander V. Mamishev (S'92–M'00) received the B.S. degree in electrical engineering from the Kiev Polytechnic Institute, Kiev, Ukraine, in 1992, the M.S. degree in electrical engineering from Texas A&M University, College Station, in 1994, and the Ph.D. degree in electrical engineering from the Massachusetts Institute of Technology, Cambridge, in 1999.

Currently, he is an Associate Professor and Director of the Sensors, Energy, and Automation Laboratory (SEAL), Department of Electrical Engineering, University of Washington, Seattle. He is the author of several technical publications. His research interests include sensor design and integration, dielectrometry, electrical insulation diagnostics, and power quality.

Dr. Mamishev is a recent recipient of the National Science Foundation CAREER Award, Outstanding IEEE Student Branch Counselor Award, and Outstanding Research Advisor Award. He is a reviewer for the IEEE TRANSACTIONS ON POWER DELIVERY and an Associate Editor for the IEEE TRANSACTIONS ON DIELECTRICS AND ELECTRICAL INSULATION.